steel research international
www.steel-research.de

# Surface Deoxidation Mechanism during Vacuum Heat Treatment of Stainless Steels AISI 304 and 446

*Cornelia Strauß, Lienhard Wegewitz,* Simon Schöler, Ulrich Holländer, Kai Möhwald, and Wolfgang Maus-Friedrichs*

**A process of removal of surface oxides from stainless steels AISI 304 and 446 that involves reduction by residual carbon, followed by the formation and desorption of carbon monoxide, is studied by investigation of thermal desorption with quadrupole mass spectrometry (QMS) and secondary ion mass spectrometry (SIMS). Carbon monoxide desorption is studied as a function of time and temperature by QMS, and carbon diffusion due to heat treatment is studied with SIMS—twice as much carbon monoxide desorbs from AISI 304 overall and desorption sets in at 900 °C as opposed to 1100 °C for AISI 446. In samples heated to 900 °C, carbon shows surface enrichment in AISI 304 but depletion in AISI 446.**

## 1. Introduction

Stainless steel surfaces are covered by tenacious oxide layers, which are composed of oxides and hydroxides of iron and chromium and other alloying elements and are only a few nanometers thick.

While it is the consensus that for successfully brazing stainless steel pieces in a vacuum furnace, it is necessary to remove the surface oxide layer, the exact processes leading to removal remain a controversial subject.

Several mechanisms are presented in the literature; a short overview is given in the following paragraphs.

Dr. C. Strauß, Dr. L. Wegewitz, Prof. W. Maus-Friedrichs
Institute of Energy Research and Physical Technologies
Technical University Clausthal
Leibnizstraße 4, Clausthal-Zellerfeld 38678, Germany
E-mail: lienhard.wegewitz@tu-clausthal.de

Dr. C. Strauß, Dr. L. Wegewitz, Prof. W. Maus-Friedrichs
Clausthal Center of Materials Technology
Technical University Clausthal
Agricolastraße 2, Clausthal-Zellerfeld 38678, Germany

S. Schöler, Dr. U. Holländer, Prof. K. Möhwald
Institute of Materials Science
Leibniz University Hannover
An der Universität 2, Garbsen 30823, Germany

The ORCID identification number(s) for the author(s) of this article can be found under https://doi.org/10.1002/srin.201900568.



**DOI: 10.1002/srin.201900568**

Keller et al. studied the wettability of several filler metals on different stainless steels.[1] In their work, they find that surface oxides of molybdenum-rich steels might be removed more easily than with other steels. Kozlova et al. concluded from there that molybdenum forms volatile suboxides during heat treatment.[2] It is therefore questionable if this applies to stainless steels in general, which may not contain molybdenum.

Chipping due to differing thermal expansion coefficients has been studied in the case of aluminum brazing in standard works by Schwartz.[3] Whether or not this takes place with passivation layers on stainless steel surfaces remains unclear, but has to be considered carefully.

Interfacial reactions can improve brazing behavior by removing wetting barriers like oxides due to the formation of new compounds at the interface.[4] This mechanism relies on the reaction between the molten braze and the steel surface within the interface of steel substrate and oxide layer. In their works, Ambrose and Nicholas presented the possibility that upon reacting, the molten braze dissolves the oxide.[5] Kang et al. used an Ag–Cu eutectic alloy with varying oxygen content as braze to join parts of stainless steel 304L. They report that at certain mass fractions of oxygen in the braze the $Cr_2O_3$ layer is destabilized, while wettability and brazing results increase.[6] Another possibility presented by McGurran and Nicholas is a diffusion-controlled undermining process of the oxide layer by the molten braze.[7]

Finally, a mechanism has been discussed which relies on the reduction of the surface layer. This reduction takes place when carbon, dissolved in the lattice of any steel, diffuses to the surface. In an early work, Arata et al. studied surface oxide removal by residual carbon.[8] They find that with the onset temperature of grain boundary formation, carbon diffuses to the surface via grain boundaries and reduces oxides present on the surface. Carbon monoxide desorption, monitored by mass spectrometry as a function of temperature, sets in at 860 °C.

Carbon monoxide desorption from stainless steel surfaces is a well-known phenomenon in other fields, i.e., the construction of ultrahigh vacuum analysis chambers. As the desorption of gas species from steel surfaces can limit the lowest attainable base pressure, thermal desorption studies have been conducted in high number. Rezaie-Serej and Outlaw studied thermal desorption from stainless steel surfaces.[9] They suggest that carbon monoxide desorption kinetic is of second order: first, diffusion of carbon to the surface, and second, the reaction of carbon with

the oxide layer, which is followed by the release of CO. This behavior was confirmed by Outlaw et al. as well.[10]

In a study related to brazing, Kozlova et al. observed the wetting behavior of stainless steel surfaces in a vacuum brazing environment.[2] Contact angles of molten silver copper eutectic on the surface of stainless steel AISI 316L were monitored with increasing temperature over time. A sudden drop in contact angle values was attributed to the onset of wetting, which was further promoted by steel surface deoxidation, leading to a further decrease in contact angle.

In a vacuum brazing furnace, the base pressure might reach $10^{-5}$ mbar, which leads to oxygen partial pressures approximately an order of magnitude lower. Based on the understanding that pressure is a gauging tool for the frequency gas particles hit a given surface, one can find that by rule of thumb, a pressure of $10^{-6}$ mbar of a given gas species leads to the formation of a monolayer of said gas species within the matter of seconds, assuming a sticking coefficient of one (see, e.g., Ertl and Küppers[11]). It can be deduced that vacuum reached in a brazing furnace might moderate oxidation, but can in no way be solely responsible for the complete reduction or removal of surface oxides.

In this work, the process of reduction of surface oxides of two stainless steels by residual carbon is studied. AISI 304 is widely spread in its applications. It is an austenitic steel containing chromium and nickel, especially singled out because it is frequently joined by means of vacuum brazing. AISI 446, in contrast, is procedurally much more demanding because of the formation of a thick aluminum oxide layer on the surface during heat treatment in brazing furnaces. Generally, ferritic steels require brazing temperatures about 100 °C higher than austenitic ones.[12] By subjecting both steels to identical heat treatments, accompanied by quadrupole mass spectrometry (QMS), differences in CO desorption behavior can be detected and compared with brazing and deoxidation behavior.

## 2. Experimental Section

### 2.1. Analytics

In this work, mass spectrometry was used in QMS and secondary ion mass spectrometry (SIMS). Both methods relied on filtering ions by their charge-to-mass ratio $m/q$.

QMS can be used to analyze gaseous species, i.e., released during thermal desorption. After ionizing, which ideally leads to singly charged ionized particles, ions have to pass through a quadrupole field. The quadrupole field can be adjusted so that only ions with specific charge-to-mass ratios can pass. With the variation of the field parameters, a spectrum as a function of $m/q$ can be recorded. Spectra directly yield the partial pressures of desorbed species. For desorption studies, a multigas analyzer with thermal (MGT) desorption by Hositrad was used. The pressure in the sample chamber reached high-vacuum range during heat treatment, around high $10^{-7}$ mbar to low $10^{-6}$ mbar, with a base pressure of around $10^{-8}$ mbar without heat treatment.

With SIMS, ions released through primary ion bombardment were analyzed. The ions released from the sample were thereafter analyzed by their $m/q$ using a QMS. By correlating bombardment or sputter time with etching depth, relative and absolute contents of elements can be determined as a function of sample depth. In this work, carbon depth profiles were determined by normalizing raw count rates with the iron count rate recorded as well. As SIMS measurements can exhibit falsified results due to surface artifacts, features of all plots were only discussed beyond a depth of 20 nm. An SIMS Workstation by Hiden was used with an $Ar^+$ primary beam of 200 nA and an acceleration voltage of 5 kV.

For imaging, a confocal laser scanning microscope (CLSM) of type VK-X210 by Keyence was used. Confocal microscopy is a scanning technique where only a small area of the inspected sample is illuminated. Solely reflected light from a small volume around the focal point was allowed to pass a pinhole aperture in the optical path. This resulted in better spatial resolution compared with ordinary light microscopes as well as stronger contrast. Furthermore, surface roughness and layer thickness can be determined by gradually shifting the focus level. The laser used as a light source operated at 408 nm wavelength.

### 2.2. Experimental Procedure

In this work, samples of both AISI 304 and 446 were investigated. Nominal compositions of both steels are shown in **Table 1**. Samples were prepared as disks, 13 mm in diameter and 2 mm thick. Sample surfaces were polished to mirror polish in aqueous diamond particle solution with a roughness depth target value of 0.02 μm. Prior to heat treatments, samples were cleaned with ethanol.

Heat treatments with the built in ceramic stage heater were conducted as follows: first, a temperature of 600 °C was held for 15 min to remove organic contamination. Then, temperature was set to 900 °C, and recording of mass spectra was started immediately. After reaching and holding 900 °C for 10 min, the temperature was set to 1100 °C. Recording of mass spectra was stopped after a temperature of 1100 °C was reached and held for 10 min. Mass spectra were recorded continuously during heat treatment, within a mass range between 10 and 30 amu to ensure short recording time. Those spectra then can be analyzed as a function of both temperature and time, with a time step of about 40 s. By correlating the variation of temperature with

**Table 1.** Nominal compositions of AISI 304 and 446, all amounts are maximum amounts in accordance to manufacturer's data.[13,14]

| Element | AISI 304 | | AISI 446 | |
|---|---|---|---|---|
| | Concentration [wt%] | Concentration [at%] | Concentration [wt%] | Concentration [at%] |
| Fe | 66.8 | 64.9 | 69.7 | 66.1 |
| Cr | 19.5 | 20.5 | 26.0 | 26.4 |
| Al | – | – | 1.7 | 3.3 |
| Ni | 10.5 | 9.8 | – | – |
| Mn | 2.0 | 2.0 | 1.0 | 1.0 |
| Si | 1.0 | 2.0 | 1.4 | 2.6 |
| C | 0.07 | 0.3 | 0.12 | 0.5 |
| N | 0.1 | 0.4 | – | – |
| P | 0.045 | 0.08 | 0.04 | 0.07 |
| S | 0.03 | 0.05 | 0.015 | 0.02 |

the variation of CO partial pressure normalized to sample chamber pressure, differences in desorption can be analyzed.

Recorded mass spectra contain nitrogen, as can be seen from the signal at 14 amu. The signal at 28 amu, therefore, does not only consist of carbon monoxide but of nitrogen as well. The fragmentation of nitrogen was deduced from spectra recorded at room temperature, so that the content of nitrogen within the 28 amu signal could be derived. Under the assumption that only hydrogen, water, oxygen, nitrogen, carbon monoxide, and carbon dioxide desorb from the sample, CO partial pressure can be derived from the spectra by eliminating nitrogen content from the signal at 28 amu. Dividing by total pressure, recorded along with temperature each time a mass spectrum is saved, yields the normalized CO partial pressure which was used to compare desorption behavior.

To study carbon diffusion behavior with SIMS, four samples were prepared. For each steel, one sample was left untreated as reference, and the other one was subjected to heat treatment performed with the stage heater of MGT. A temperature of 900 °C was set and held for 10 min; afterward, samples were transported to SIMS work station. Both samples were treated simultaneously to ensure identical conditions.

## 3. Results

### 3.1. Nitrogen Fragmentation

Nitrogen fragmentation was deduced by recording spectra at room temperature with negligible signal at 12 amu. It was found that the signal at 14 amu was 13.28% of the signal at 28 amu. This value coincides quite well with what can be found with the help of nitrogen mass spectra in NIST database (13.79%).

CO partial pressure was then determined by dividing the values at 14 amu by 0.1328, and then subtracting these values from the signals at 28 amu.

### 3.2. Comparison of CO Desorption

Representative plots of CO desorption as a function of time are shown for each steel in **Figure 1** and **2**, respectively. All axes have been set to the same range to facilitate comparison.

Normalized CO partial pressure as a function of time is plotted in black, referring to the axis on the right, whereas temperature as a function of time is plotted in gray. The dashed line refers to the actual temperature, measured each time a spectrum is recorded, whereas the solid line represents the set temperature, which refers to the temperature regimen described earlier. Temperature axis is on the left.

As can be seen, AISI 304 shows CO desorption in the temperature range around 900 °C and peaks after increasing the temperature to 1100 °C. AISI 446 manifests little to no desorption in the lower temperature range, with desorption setting in after increasing the temperature to 1100 °C.

By integrating CO partial pressure curves of all measurements, overall desorption was compared for AISI 304 and 446, yielding a mean ratio of 2:1. Comparing desorption maxima at 1100 °C yields a mean ratio of 1.5:1.

As desorption peaks for both steels after setting the temperature to 1100 °C, onset times were determined by extrapolating the slopes of both actual temperature and CO partial pressure to the time axis. Results are shown in **Table 2**. It can be seen that on average, AISI 304 reaches the desorption maximum in half the time compared with AISI 446.

### 3.3. Carbon Depth Profiles

Normalized carbon depth profiles determined by SIMS are shown in **Figure 3**. Carbon depth profiles for both heated samples are compared over a depth of 2 µm, where the black line refers to AISI 304 and the green line refers to AISI 446.

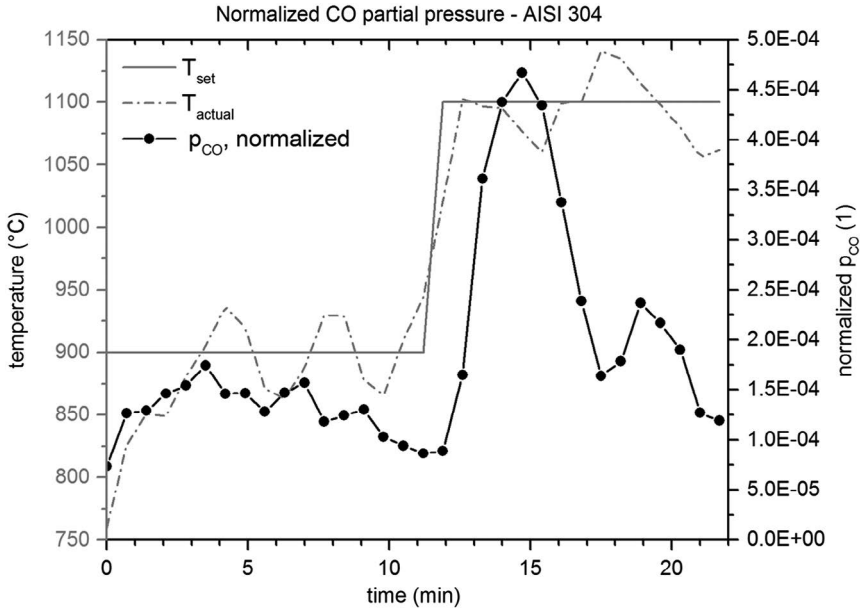


**Figure 1.** Normalized CO partial pressure during heat treatment of AISI 304.

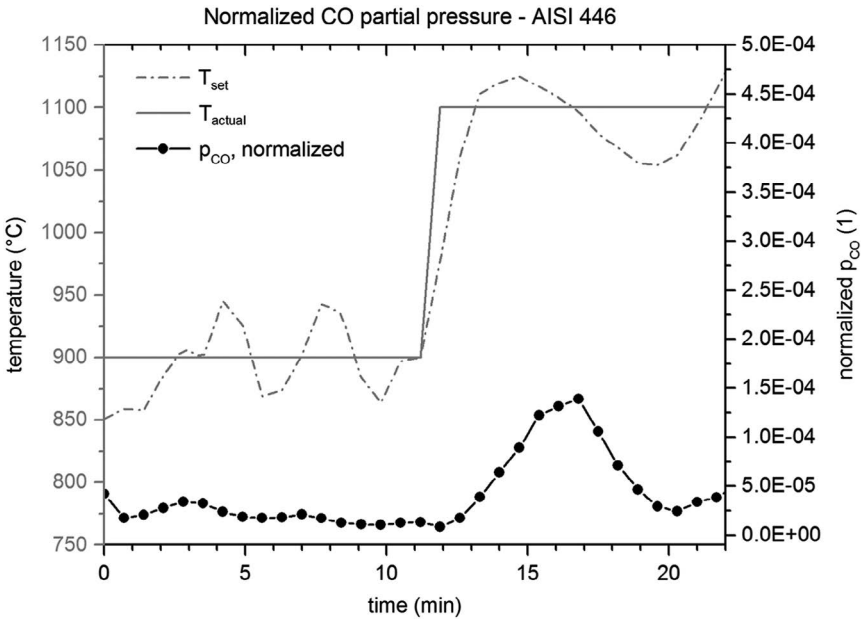


**Figure 2.** Normalized CO partial pressure during heat treatment of AISI 446.

**Table 2.** Comparison of onset times to reach the maximum of CO desorption.

| AISI 304 | | AISI 446 | |
|---|---|---|---|
| Onset time [min] | | Onset time [min] | |
| Sample 1 | 1.5 | Sample 1 | 2.7 |
| Sample 2 | 1.2 | Sample 2 | 2.8 |
| Sample 3 | 1.9 | Sample 3 | 3.4 |
| Mean | $1.5 \pm 0.2$ | Mean | $3.0 \pm 0.2$ |

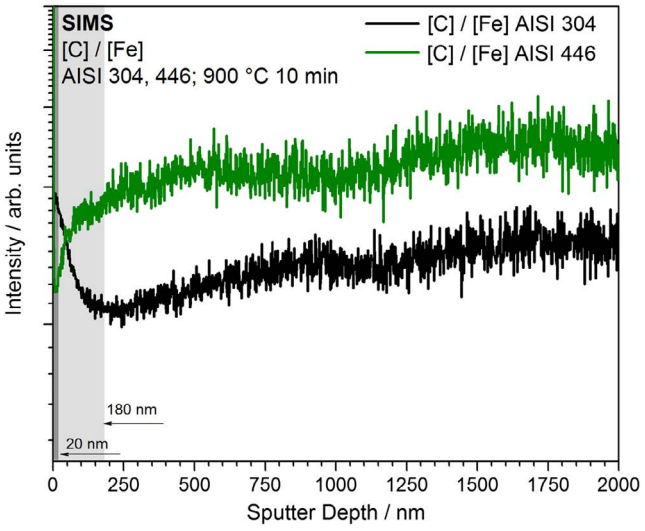


**Figure 3.** Carbon depth profiles of AISI 304 (black line) and AISI 446 (green line) heated at 900 °C.

In direct comparison of both steels, a drastically different behavior can be detected. For AISI 304, surface enrichment of carbon down to a depth of around 180 nm can be observed. The trend is opposed for AISI 446, exhibiting a surface depletion of carbon in the first 180 nm.

In **Figure 4** and **5**, grain structures of AISI 304 and 446, respectively, in untreated state are shown by CLSM images taken in the SIMS etching spot. After high-energy ion impact, the previously polished surface is etched in a spot roughly $250 \times 250\ \mu m^2$, which allows imaging of the grain structure. As can easily be seen, grain size differs drastically. Smaller grains, as exhibited by AISI 304 (Figure 4), lead to a higher volume ratio of grain boundaries to grains as opposed to larger grains exhibited by AISI 446.

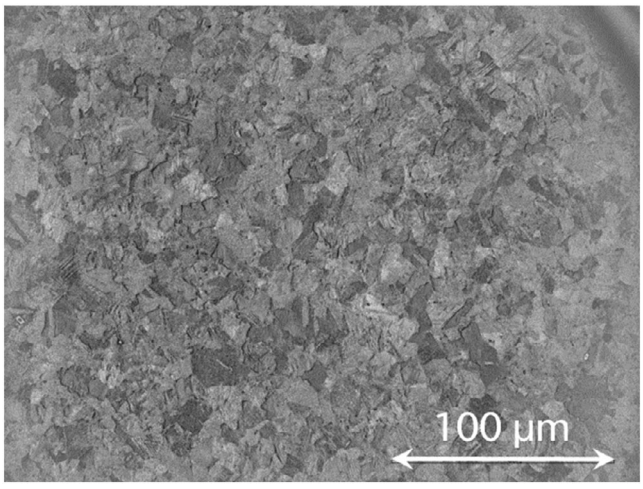


**Figure 4.** CLSM image of grain structure of untreated AISI 304, revealed in the SIMS measurement spot.

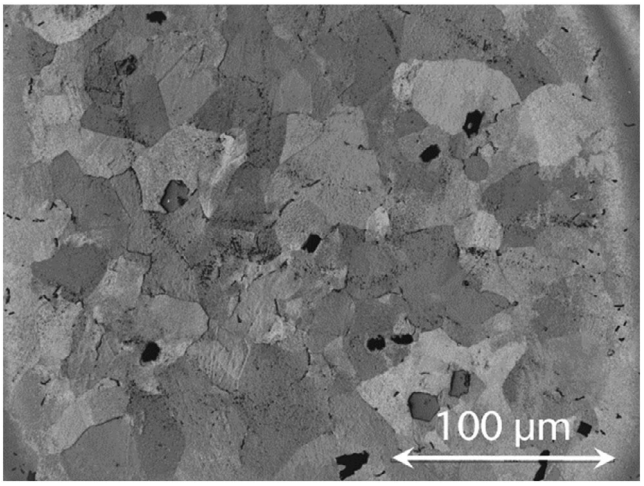


**Figure 5.** CLSM image of grain structure of untreated AISI 446, revealed in the SIMS measurement spot.

## 4. Discussion

With AISI 446, CO desorption does not set in until increasing the temperature to 1100 °C. In contrast, AISI 304 shows CO desorption around 900 °C that peaks after increasing the temperature to 1100 °C. On average, the desorption maximum is 1.5 times higher than the desorption maximum manifested by AISI 446. Overall desorption, determined by integrating CO partial pressure curves, is 2 times higher for AISI 304 than for AISI 446.

As onset times (see Table 2) differ as well, it is possible to conclude that with AISI 304, the desorption process sets in around 900 °C. Increasing the temperature to 1100 °C then amplifies desorption, which is already taking place, as carbon diffusion is thermally activated. For AISI 446, in contrast, desorption sets in around 1100 °C.

As can be ascertained by SIMS measurements, carbon depth profile trends differ drastically for both steels. In direct comparison of carbon depth profiles recorded of both heated samples, it can be seen that AISI 304 shows surface enrichment down to depths of 180 nm, which cannot be observed for AISI 446. It can be concluded that carbon diffusion to the surface of AISI 304 takes place in the temperature range where this steel already shows CO desorption. No carbon surface enrichment can be observed for AISI 446, which matches well with little to no CO desorption taking place at 900 °C. Due to identical conditions in heat treatment, this points to differences in carbon diffusion behavior.

Grain boundaries might play an important role. AISI 304 displays smaller grains, thus presenting a higher volume ratio of grain boundaries to grains than AISI 446. Grain boundaries are known to facilitate diffusion, notably carbon diffusion.[15] It is, therefore, possible that carbon diffusion can take place at a higher rate for AISI 304, but does not yet for AISI 446.

In earlier work, it has been shown that depending on the surrounding pressure, aluminum oxide forms on the surface of AISI 446. During heat treatment in a vacuum brazing furnace (maximum temperature of 1150 °C, base pressure around $10^{-5}$ mbar), a thick aluminum oxide layer of several 100 nm is formed on the surface. Yet, during heat treatment under ultra-high vacuum conditions (base pressure around $10^{-9}$ mbar, maximum temperature of 1200 °C), no aluminum is detected on the surface, but rather carbides of foreign elements like titanium or vanadium.[16] Those carbon affine elements, detected repeatedly when analyzing AISI 446, could further limit carbon diffusion due to chemical trapping.

Differences in carbon diffusion could also be explained with different amounts of soluble carbon in austenitic and ferritic lattice, respectively. According to Ishigami et al., a lack of solute carbon as present in ferritic steels in comparison with austenitic steels entails the need for lower surrounding pressure and/or higher temperatures in order for surface oxide reduction to occur.[17] The conclusion is drawn that austenitic steels are more easily reduced than ferritic ones, as is stated by Holländer et al. as well.[12]

It is well established that some stainless steels are not as easily brazed as others; differences in carbon diffusion might explain that. One has to remain careful, however, when stating that enabling carbon monoxide desorption, e.g., by lowering the pressure or even only the CO partial pressure of the surrounding atmosphere, leads to oxide-free surfaces and thus successful brazing processes. First, it still remains unclear whether a surface has to be completely oxide free down to molecular level to carry out a successful brazing process. Second, carbon monoxide desorption might result from the equilibrium of two opposed processes: reduction of oxides, yielding CO desorption, and surface oxidation due to high oxygen partial pressures in a brazing furnace. In the case of AISI 446, it is well known that aluminum oxide forms during heat treatment in a brazing furnace. It is still possible that some of that oxide layer gets partially reduced by carbon, as is stated, e.g., by Lugscheider et al.[18] This would mean that if carbon monoxide desorption takes place, it may not be sufficient to ensure an oxide-free surface.

## 5. Conclusions

AISI 304 desorbs more CO overall than AISI 446, and at lower temperatures. This mirrors surface deoxidation behavior and brazing behavior as well, as AISI 304 can generally be successfully brazed at lower temperatures than AISI 446.

Carbon diffusion behavior, studied by SIMS at 900 °C, matches CO desorption behavior of both steels in this temperature range, showing surface enrichment for AISI 304 but not for AISI 446.

It is, therefore, possible that the mechanism leading to oxide-free surfaces or sufficiently oxide-free surfaces in a vacuum brazing process relies on carbon diffusion to the surface with subsequent reduction of surface oxides and desorption of carbon monoxide. It remains unclear whether CO desorption taking place is sufficient for successful brazing processes.

Further diffusion studies with SIMS have to be conducted to gain better understanding of diffusion mechanisms in both steels, e.g., by varying temperature and holding time of heat treatments. The role of carbon affine foreign elements found in AISI 446, possibly acting as diffusion sinks for carbon, should then be investigated as well.

Finally, other factors contributing to wettability like surface morphology should be studied, like capillary effect of grain boundaries as is manifested in grain boundary infiltration.

## Acknowledgements

The authors would like to thank Michal Schultz for SIMS measurements and the German Research Foundation (DFG) for financial support (grant nos. MA 1893/24-1 and MO 881/22-1).

## Conflict of Interest

The authors declare no conflict of interest.

## Keywords

stainless steels, surface deoxidation, surface oxide removal, vacuum brazing, wetting

Received: October 28, 2019
Revised: December 22, 2019
Published online: January 21, 2020

[1] D. L. Keller, M. M. McDonald, C. R. Heiple, W. L. Johns, W. E. Hofmann, *Weld. J.* **1990**, *69*, 31.
[2] O. Kozlova, R. Voytovych, M.-F. Devismes, N. Eustathopoulos, *Mater. Sci. Eng. A* **2008**, *495*, 96.
[3] M. M. Schwartz, *Brazing*, ASM International, Materials Park **2003**.
[4] O. Dezellus, N. Eustathopoulos, *J. Mater. Sci.* **2010**, *45*, 4256.
[5] J. C. Ambrose, M. G. Nicholas, *Mater. Sci. Technol.* **1996**, *12*, 72.
[6] Y. Kang, J. Han, H. Kim, J. Lee, *J. Mater. Sci.* **2016**, *51*, 1713.
[7] B. McGurran, M. G. Nicholas, *Brazing Soldering* **1985**, *5*, 43.
[8] Y. Arata, A. Ohmori, H. Fu Cai, *Trans. JWRI* **1983**, *12*, 27.
[9] S. Rezaie-Serej, R. A. Outlaw, *J. Vac. Sci. Technol. A* **1994**, *12*, 2814.
[10] R. A. Outlaw, X. Zhao, B. C. Holloway, M. R. Davidson, E. Lambers, *Appl. Surf. Sci.* **2004**, *227*, 7.
[11] G. Ertl, J. Küppers, *Low Energy Electrons and Surface Chemistry*, VCH Verl. Ges., Weinheim **1985**.
[12] U. Holländer, D. Wulff, A. Langohr, K. Möhwald, H. J. Maier, *Int. J. Precis. Eng. Manuf. Green Technol.* **2019**, 1, https://doi.org/10.1007/s40684-019-00109-1.
[13] METALCOR, Specification Sheet AISI 304, http://www.metalcor.de/en/datenblatt/5 (accessed: December 2019).
[14] METALCOR, Specification Sheet AISI 446, http://www.metalcor.de/en/datenblatt/54 (accessed: December 2019).
[15] H. Mehrer, *Diffusion in Solids: Fundamentals, Methods, Materials, Diffusion-Controlled Processes*, Springer, Heidelberg, Berlin **2007**.
[16] C. Strauß, R. Gustus, W. Maus-Friedrichs, S. Schöler, U. Holländer, K. Möhwald, *J. Mater. Process. Technol.* **2019**, *264*, 1.
[17] I. Ishigami, E. Tsunasawa, K. Yamanaka, *Trans. Jpn. Inst. Met.* **1981**, *22*, 337.
[18] E. Lugscheider, H. Zhuang, M. Maier, *Weld. J.* **1983**, 295.